Unraveling the Molecular Basis of Subunit Specificity in P Pilus Assembly by Mass Spectrometry

Rebecca J. Rose[1], Denis Verger[2], Tina Daviter[2], Han Remaut[2], Emanuele Paci[1], Gabriel Waksman[2,3*], Alison E. Ashcroft[1*], Sheena E. Radford[1*]

[1]Astbury Centre for Structural Molecular Biology and Institute of Molecular and Cellular Biology, University of Leeds, Leeds, LS2 9JT, United Kingdom
[2]Institute of Structural Molecular Biology at UCL/Birkbeck and School of Crystallography, Malet Street, London WC1E 7HX, United Kingdom
[3]Research Department of Structural and Molecular Bioscience, University College London, Gower Street, London WC1E 6BT, United Kingdom

*To whom correspondence should be addressed.

Abstract

P pili are multi-subunit fibers essential for the attachment of uropathogenic *Escherichia coli* to the kidney. These fibers are formed by the non-covalent assembly of six different homologous subunit types in an array that is strictly defined in terms of both the number and order of each subunit type. Assembly occurs through a mechanism termed "donor-strand exchange (DSE)" in which an N-terminal extension (Nte) of one subunit donates a β-strand to an adjacent subunit, completing its immunoglobulin fold. Despite structural determination of the different subunits, the mechanism determining specificity of subunit ordering in pilus assembly remained unclear. Here we have employed non-covalent mass spectrometry to monitor DSE between all 30 possible pairs of P pilus subunits and their Ntes. We demonstrate a striking correlation between the natural order of subunits in pili and their ability to undergo DSE *in vitro*. The results reveal new insights into the molecular mechanism by which subunit ordering during the assembly of this complex is achieved.

Introduction

Gram-negative bacteria assemble a variety of surface organelles to mediate recognition and attachment to host tissues (1, 2). These pili or fimbriae are multi-subunit filamentous appendages that typically present an adhesin at their tip that binds to a specific host receptor and is essential for infectivity (3, 4). Pili are formed by at least four known pathways in Gram-negative bacteria, one of which, the chaperone-usher pathway, assembles a large number of adhesive pili essential for pathogenesis (5). In this pathway, pilus subunits are synthesized in the cytoplasm and transported, *via* the Sec machinery, into the periplasm (2). Here, the same periplasmic chaperone binds each subunit, capping its interactive surfaces and maintaining it in an assembly-competent conformation (Figure 1a) (6-8). The chaperone-subunit complexes are then taken to a site of assembly consisting of an outer-membrane protein, the "usher", where the chaperone is released and subunit polymerization occurs (Figure 1a) (9).

The structures of the chaperones and pilus subunits ('pilins') have been solved for several chaperone-usher pilus systems (10). The chaperone consists of two immunoglobulin (Ig)-like domains (11). In the periplasm, each pilus subunit forms an incomplete Ig fold, in which the C-terminal β-strand is absent. This leaves a hydrophobic groove into which the chaperone inserts the G strand of its domain 1 (strand G_1), completing the subunit's fold (Figure 1b,c) (12-15). In this binding interface, four residues from the donated chaperone β-strand (named P1-P4 residues, see below) insert into complementary hydrophobic pockets (named P1-P4 pockets) formed within the pilin groove, leaving another pocket (P5) in the groove exposed (Figure 1c). This interaction is known as "Donor-Strand Complementation" (DSC). With the exception of the adhesin, each subunit also possesses an unstructured N-terminal extension (Nte), usually more than 11 residues in length that is not involved in its Ig-like fold (Figure

1b). This region contains a conserved binding motif of alternating hydrophobic residues (named P2-P5 residues) (Figure 1d). In the interaction between two subunits, as in the polymeric pilus itself, the Nte from one subunit occupies the hydrophobic groove of an adjacent subunit, binding to the P2-P5 pockets and completing its Ig fold (Figure 1e,f) (8, 14, 15). The reaction whereby the chaperone's strand is exchanged with the Nte of the subunit next in assembly is termed "Donor-Strand Exchange" (DSE).

The P pilus is a prototypic chaperone-usher system, assembled by uropathogenic *Escherichia coli* and encoded by the *pap* (pyelonephritis-associated pilus) operon. P pili are highly complex fibers, composed of six different subunit types that are assembled in a specific order (Figure 1a) (3, 16-18). Subunit ordering in these pili is highly conserved and likely to be important for preserving optimal function and hence the pathogenicity of the bacterium (4, 17). The first subunit to be assembled is a single copy of PapG, an adhesion molecule or "adhesin", that binds Galα(1-4)Gal moieties on kidney tissue and is necessary for establishing infection (19). This is followed by a single copy of an adaptor subunit, PapF, the incorporation of which precedes assembly of approximately ten copies of PapE, which forms the bulk of the flexible tip fibrillum. Subsequent incorporation of a single copy of another adaptor subunit, PapK, leads to the incorporation of thousands of PapA subunits that form the rigid helical PapA rod. Finally, pilus biogenesis is halted by the incorporation of a single copy of the termination subunit PapH (Figure 1a) (18).

Despite the importance of controlled subunit ordering for the production of functional pili, how the incorporation of correct subunits is coordinated during pilus biogenesis remains an open question. Differences in affinity between the various chaperone-subunit complexes and the usher could contribute to subunit ordering since the PapD:PapG and PapD:PapF

complexes exhibit the highest affinity for the PapC usher (9, 20). On the other hand, the interaction of the Nte with the acceptor groove may also play a role in determining subunit ordering. Indeed, a recent mutagenesis study of the PapF subunit has demonstrated that its Nte sequence is crucial for the interaction of PapF with PapG and its function as an adaptor subunit (21). However, the role of Nte:groove interactions in determining subunit:subunit recognition in the Pap system has never been comprehensively explored. Here, we have used non-covalent mass spectrometry (MS) (22) to perform a systematic study of all 30 possible pairwise interactions between the six Pap subunits with the five Ntes of PapF, PapE, PapK, PapA and PapH (Figure 1a,d). Despite the high structural homology of the Pap subunits (8, 12, 18, 23), and the conserved binding motifs of all Ntes (Figure 1d), we show dramatic differences in the reactivity between different subunit:Nte pairs that mirror closely the order of subunit assembly found in the assembled pilus. The data provide new insights into the origins of subunit ordering in pilus formation, suggesting that specificity is determined, at least in part, by the interaction between the Nte sequence and the acceptor binding groove and that, within this interaction, the sequence of the Nte at and around the P5 residue is of particular importance.

Results

Donor-strand exchange monitored by non-covalent MS

In order to examine the specificity of DSE in Pap assembly, an *in vitro* assay was established in which all six chaperone:subunit complexes were incubated individually in the presence of peptides corresponding to each of the five Pap Ntes (Figure 1d). PapG lacks an Nte since it is positioned at the distal end of the pilus and acts only as a donor-strand acceptor (Figure 1a). For reactions involving PapE or PapA, the only two self-polymerizing subunits, truncated constructs were used to prevent self-polymerization. In PapE, the entire Nte was removed, creating $PapE_{Ntd1}$ (8), for PapA, the region N-terminal to the conserved Nte binding sequence was removed, and the conserved glycine at the P4 site was substituted with Asn, creating $PapA_{Ntd1G15N}$ (23). These constructs have been shown not to self-polymerize and to be suitable models as donor-strand acceptors (8, 23). A stable PapH construct, referred to as $PapH_{Ntd1}$, was used whereby the proline-rich N-terminal region of the Nte, known not to be involved in DSE, was removed (18). Previous studies have established the validity of adding peptides *in trans* to mimic DSE: Lee *et al.* showing *in vivo* that the Nte and Ig-folded domain function separately in the Pap system, while Remaut *et al.* demonstrated that the relative rate of DSE initiated by different Nte peptides in Saf pilins from *Salmonella enterica* mirrored that of their intact subunit counterparts (15, 21).

Of the 30 reactions examined, seven mimic the interactions known to occur in the pilus structure *in vivo* (referred to hereafter as 'cognate' interactions) whilst the remaining 23 reactions involve non-cognate pairings. A ten-fold molar excess of peptide over chaperone:subunit complex was chosen as the optimal concentration ratio (see SI Methods). Under these conditions DSE proceeds with pseudo-first order kinetics, allowing the reactivity

of different Nte:subunit pairs to be compared. In each case the progress of the reaction was monitored by non-covalent nano-electrospray ionization MS (nanoESI-MS) (15, 22).

Mass spectra of the reactions between PapD:PapK (theoretical mass 42,224.8 Da, experimental mass 42,225.9 Da) and the Nte peptide of PapA (A_{Nte}, cognate) or the Nte peptide of PapK (K_{Nte}, non-cognate) are shown as examples in Figure 2. Individual components within the sample mixtures were identified by their unique mass (accuracy <0.01%), confirmed by the presence of a minimum of three consecutive charge state peaks (see Methods). The ESI mass spectra of PapD:PapK shortly after addition of each Nte (Figure 2a and e) show PapD:PapK to be the predominant species (red peaks). However, with time, changes in the spectra reveal the progress of DSE, with the peaks corresponding to PapD:PapK decreasing in intensity, and new charge state distributions relating to the PapK:A_{Nte} or PapK:K_{Nte} complexes (blue peaks) and released PapD (yellow peaks), the products of DSE, appearing and increasing in intensity (Figure 2b,c,f,g). Integration of the peaks from each spectrum showed a marked difference in the progression of DSE for the cognate and non-cognate pairs (Figure 2d,h). Thus, whilst the reaction between PapD:PapK and A_{Nte} is effectively complete within 72 hr, a significant amount of the PapD:PapK complex remains in the reaction with K_{Nte} at this time, with only small peaks relating to the PapK:K_{Nte} product observed (Figure 2g). The data demonstrate the effectiveness of nanoESI-MS to monitor DSE in real-time, allowing the potentials of different cognate/ non-cognate pairs to undergo DSE to be compared.

Chaperone:subunit complexes react preferentially with cognate Ntes

The ability of each chaperone:subunit complex to undergo DSE with each peptide Nte, monitored using nanoESI-MS, is shown in Figure 3. The results reveal a striking span of

reactivities, with the most rapid reactions reaching completion within 20 hr (PapD:PapE$_{Ntd1}$ plus K$_{Nte}$ or E$_{Nte}$) (Figure 3c), while other combinations showed no significant reaction even after 300 hr (e.g. PapD:PapG plus H$_{Nte}$, A$_{Nte}$, K$_{Nte}$ or E$_{Nte}$ (Figure 3a)). With the exception of PapD:PapH$_{Ntd1}$, which does not undergo DSE with any Nte, consistent with the role of this subunit in capping assembly (Figure 3f) (18), all other chaperone:subunit complexes were able to undergo DSE.

Interestingly, individual chaperone:subunit complexes showed different reactivities with each Nte, with some complexes being highly specific for their cognate Ntes (e.g. PapD:PapG, Figure 3a) while others were more promiscuous (e.g. PapD:PapF, Figure 3b). To compare the reactivity of each chaperone:subunit complex for each Nte, the progress of DSE (measured by chaperone:subunit loss) was fitted to a single exponential function (see SI Methods), yielding an apparent rate constant, k_{obs}, for each chaperone:subunit/ Nte pair (Figure 3g-k and SI Table 1). The results reveal a striking correlation of the apparent rate of DSE with the nature of the Nte (cognate or non-cognate), with the most rapid reactions uniformly occurring with the cognate partner(s). The data suggest, therefore, that the complementarity between each subunit groove and its cognate Nte plays a significant role in determining subunit assembly.

The apparent rate of DSE for each chaperone:subunit complex with its cognate Nte is compared in Figure 4. The figure highlights the wide range in k_{obs} for the different cognate pairs, ranging from 2.1×10^{-1} hr^{-1} for PapD:PapE$_{Ntd1}$ plus K$_{Nte}$ to 5.5×10^{-3} hr^{-1} for PapD:PapG plus F$_{Nte}$. Interestingly, the slowest two reactions occur for PapG and its adaptor PapF, both of which are essential for pilus function (17, 21) and have the highest affinity for the usher protein (9, 20). By contrast, the subunits that self-polymerize *in vivo* (PapE and PapA) show some of the most rapid rates of DSE.

Subunit reactivity is determined by complementarity at the P5 pocket

The range of reactivities between different chaperone:subunit Nte pairs is remarkable given the structural homology between the subunit folds (mean C_α RMSD = 2.0Å, see SI) and the highly conserved Nte binding motif, comprised of the P2 to P5 residues of the different Ntes (Figure 1d). Despite the close similarity of the different Nte sequences (Fig. 1d) the subunits themselves differ significantly in sequence (overall similarity of ~25% (see SI Fig. S1). Previous studies of DSE in the Saf pilus system demonstrated a key role for the P5 residue in the Nte and the P5 pocket in the subunit groove in determining the rate of DSE (15). To determine whether this is also the case in the P pili examined here, different chaperone:subunit complexes were challenged with chimeric Nte peptides, comprised of the N-terminal half of a cognate Nte (encompassing the P2 and P3 residues) and the C-terminal half of a non-cognate Nte (encompassing the P4 and P5 residues) and *vice versa*, and the reactivity of each was examined using nanoESI-MS. Since the P4 residue is a conserved glycine in all Ntes, only the P5 site and adjacent residues differ in the C-terminal region (Figure 1d) and hence these chimeric peptides serve as a good model to determine the role of this region in determining chaperone:subunit/ Nte reactivity. Two chaperone:subunit complexes were chosen for analysis, the rapidly reacting PapD:$PapE_{Ntd1}$ and the more slowly reacting PapD:PapF (Figure 3b,c). PapD:$PapE_{Ntd1}$ was incubated with chimeric peptides comprised of the N-terminal half of E_{Nte} and the C-terminal half of H_{Nte} (named E/H_{Nte}), as well as the complementary peptide H/E_{Nte}. These peptides were carefully chosen to represent a cognate (E_{Nte}) and a non-cognate (H_{Nte}) Nte that react rapidly and slowly, respectively (Figure 3c,i). Similarly, PapD:PapF was incubated with E/K_{Nte} and K/E_{Nte} (Figure 3b,h). The progress curves of these reactions (Figure 5) showed that the apparent rate of DSE is determined by the C-terminal half of the Nte. Thus, DSE of PapD:$PapE_{Ntd1}$ with E/H_{Nte}

mirrors that of H_{Nte}, whilst H/E_{Nte} mirrors E_{Nte} (Figure 5a). Similar results were obtained for PapD:PapF, with K/E_{Nte} mirroring E_{Nte}, and E/K_{Nte} mirroring K_{Nte} (Figure 5b). The results demonstrate that residues at, or adjacent to, the P5 site play a key role in determining Nte-groove reactivity in P pili, the Nte presumably then zipping into the complementary groove in a mechanism that is likely conserved in all pili belonging to this family (15, 24).

Discussion

P pili possess a complex architecture involving the precise ordering of a well-defined number of six different subunit types. Despite detailed structural studies of different chaperone:subunit and subunit:Nte complexes (10), how the correct assembly of this complex organelle, which is essential for the virulence of a number of pathogenic Gram-negative bacteria (5), is determined has remained unclear. In a recent study of the PapF adaptor, the Nte of PapF was shown to be essential to assemble functional pili, although the PapG:PapF:PapE order could be altered to a PapG:PapE order simply by replacing the Nte of PapE with that of PapF in the PapE subunit (21). However, how subunit ordering is achieved *in vivo*, whether this can be emulated in DSE reactions *in vitro* and the molecular basis of subunit discrimination have not been explored systematically. Here, using non-covalent nanoESI-MS and experiments that mimic DSE *in vitro*, we provide evidence of an inherent specificity between different pairs of acceptor subunit grooves and donor subunit Ntes that mirrors subunit order in the intact pilus. Thus, all subunits located adjacently in P pili (cognate pairs) react more rapidly than their associated non-cognate pairs (Figure 3). The results suggest that the inherent compatibility of each Nte for each subunit groove plays an important role in determining the order of subunit assembly *in vitro.*

A further important feature of DSE to emerge from this study is the exquisite sensitivity of the reaction to sequence changes. Thus the chimeric peptides H/E_{Nte} and E/H_{Nte} share 66% and 60% sequence identity with E_{Nte} and H_{Nte}, respectively, yet show apparent rates of DSE with PapD:$PapE_{Ntd1}$ that differ markedly (Figure 5). Given that the P4 site is a conserved Gly in all five Ntes studied here, the data demonstrate that residues at, or close to, the P5 site play a significant role in determining subunit:Nte reactivity. Similar results have been observed for Saf, in which single amino acid substitutions at the P5 site result in significant alterations in

the rate of DSE (15). It is likely that residues adjacent to the one that inserts into the P5 pocket are also important, potentially due to interactions formed at the surface of the pocket. However, the precise structural basis for the rate differences is unknown, and future kinetic analyses combined with structures of all six subunits will be needed to determine the importance of individual residues in determining subunit ordering. Co-evolution of the pilin genes within the pilus operon has thus resulted in a family of pilins in which the complementarity between binding grooves and their cognate Nte sequences are finely tuned so as to enable subtle changes in sequence to influence subunit:subunit interactions.

The ability of chaperone:subunit complexes to undergo DSE *in vitro* with non-cognate Ntes, albeit less efficiently than their cognate counterparts, could provide an evolutionary advantage for subunit assembly *in vivo*, enabling the development of new pilus sequences and preventing mutations from ablating the ability of a pathogenic bacterium utilizing the chaperone-usher system to export these essential virulence factors. For example, pili grown in *E.coli* that lack a *papK* gene are able to assemble with the usual architecture of a tip fibrillum and a rod, but the fibrillae in these bacteria are approximately twice as long as those found in wild-type pili (3). This suggests that the order of assembly must be altered in these pili, with PapE undergoing DSE with A_{Nte}, rather than the usual cognate reaction with K_{Nte} (Figure 1a). The increased length of the fibrillum in the *papK*$^{-}$ bacteria is consistent with the slower rate of DSE observed here *in vitro* for PapD:PapE with A_{Nte} compared with K_{Nte} (Figure 3). The data suggest, therefore, that functional pili with different orders and numbers of subunits can be assembled *in vivo*, although some architectures will be more favoured by the inherent complementarity of different subunit:Nte pairings.

While our results demonstrate the importance of the groove:Nte interactions in determining subunit:subunit interactions *in vitro*, other factors play a role in determining subunit ordering during pilus assembly *in vivo*. Firstly, as in any multi-molecular interaction, the rate of subunit incorporation during pilus assembly *in vivo* will depend on the concentration of each reaction partner. Secondly, the usher itself may play a role in determining subunit ordering. Indeed, the usher is known to bind chaperone:subunit complexes with different affinities (9, 20), which could increase the probability of incorporation of some subunits over others.

The observation that pilus formation occurs more rapidly *in vivo* (minute timescale) (25), compared with the timescale of DSE observed here *in vitro*, suggests an active role for the usher in subunit polymerization. Indeed, recent experiments have shown that the FimD usher of Type I pili acts as a catalyst of DSE (26). The recently solved crystal structure of the PapC usher, combined with cryo-electron microscopy images of the FimD usher caught in the act of DSE, suggest a structural rationale for the catalytic power of the usher, whereby the two periplasmic N-terminal domains of the usher dimer alternately recruit chaperone-subunit complexes for pilus assembly, most probably bringing them into close proximity with previously assembled subunits in the usher pore and orienting them optimally for DSE (27). However, while such a proximity effect may provide a rationale for the observed catalytic effect of the usher on DSE, the extent to which the usher actively modulates or controls subunit ordering remains elusive.

Methods

Protein Expression and Purification

Details of the cloning of different *pap* genes and the expression and purification of chaperone:subunit complexes are described in SI.

N-terminal Extension Peptides

Peptides representing the Ntes of PapH, PapA, PapK, PapE, PapF, plus hybrid E/K_{Nte}, K/E_{Nte}, E/H_{Nte} and H/E_{Nte} peptides, were purchased from CSS Albachem, Gladsmuir, UK. The peptides were dissolved in 5mM ammonium acetate, pH 5.5. Two lysine residues were added C-terminally to each Nte sequence (not shown in Figure 1d) to increase solubility. The C-terminus of each peptide was amidated. Control experiments comparing the rates of DSE using the A_{Nte} or H_{Nte} peptides with and without the additional Lys-Lys sequence, confirmed that these residues do not affect the kinetics of DSE (data not shown).

Mass Spectrometry Data Acquisition and Processing

40μM of each chaperone:subunit complex was incubated individually with 400μM of each Nte peptide in 5mM ammonium acetate, pH 5.5 at 22ºC. The temperature and pH were optimized to minimize complex dissociation during data acquisition and to allow sufficient data to be collected over an appropriate time period. The reactions were sampled from an initial time point of *ca.* 1 min after addition of the peptide Nte to 14 days, and analyzed using a Q-Tof1 mass spectrometer with a nanoESI source (Waters UK Ltd., Manchester, UK) (see SI for further details).

MS data were processed using the MassLynx software supplied with the Q-Tof1 (see SI Methods). The areas of all peaks (including salt adducts) for a given species were summed

and expressed as a fraction of the total area under all peaks in the spectrum. For quantitative analysis, the chaperone:subunit loss data were then normalized between the maximum concentration (i.e. concentration of reactant before reaction initiation) and the baseline signal (for more details see SI Methods). Analysis of triplicate reactions showed a standard deviation of ±2.5%, demonstrating the high reproducibility of the experiment. Data were fitted to a single exponential, assuming that each reaction goes to completion, to give an apparent rate constant of DSE (k_{obs}). Where less than 20% of the chaperone:subunit complex had reacted after 14 days, an upper limit for k_{obs} was estimated (see SI).

Acknowledgements

We acknowledge with thanks Scott Hultgren for inspirational discussions on pilus assembly, and Toshana Foster for supporting work. RJR was funded by a BBSRC/CASE PhD studentship and Waters UK Ltd.. We thank Dr R.H. Bateman (Waters UK Ltd.) for continued support. The Q-Tof1 mass spectrometer was funded by the BBSRC. The work was supported with funds from the BBSRC and the Wellcome Trust.

Figure Legends

Figure 1. The P pilus, DSC and DSE complexes and conserved Nte binding sequences. **(a)** Schematic diagram of P pilus biogenesis. Subunits (coloured), bound to a chaperone (PapD, brown) in the periplasm, assemble at the usher (PapC, grey) in the order PapG, PapF, PapE, PapK, PapA and PapH. **(b)** Topology diagram of the DSC interaction. In this complex the chaperone G_1 strand (brown) completes the Ig fold of each subunit (green) by binding into the hydrophobic groove between strands A and F (indicated). The Nte is unstructured. **(c)** Crystal structure of the DSC interaction between the subunit PapK (shown in space fill) in complex with the chaperone PapD (brown) [PDB file 1PDK]. The P1-P4 residues and the exposed (unoccupied) P5 pocket are indicated. **(d)** Sequences of Ntes of different Pap subunits. Full-length Ntes were used for PapA, PapK, PapE and PapF, whereas the long N-terminus of the Nte of PapH (which does not participate in donor-strand exchange (18)) was truncated to aid solubility. The peptides used in this study to mimic each Nte (see Methods) are outlined in black. Residues composing the hydrophobic binding motif (P2-P5) are shown in red. **(e)** Topology diagram of the DSE interaction. The Nte from one subunit (green) completes the Ig fold of the subunit previously assembled (yellow) by forming a new intermolecular β-strand. **(f)** Crystal structure of the subunit PapE (shown in space fill) bound to the Nte of PapK (green) [PDB file 1N12]. The P2-P5 residues that bind to the P2-P5 pockets are indicated.

Figure 2. ESI-MS of cognate/ non-cognate DSE reactions. NanoESI mass spectra of the DSE reactions between PapD:PapK and **(a-c)** A_{Nte} and **(e-g)** K_{Nte}: **(a,e)** 30 min, **(b,f)** 24 hr and **(c,g)** 72 hr after reaction initiation. Chaperone:subunit complex is shown in red, unbound chaperone in yellow, and subunit:Nte product in blue. **(d,h)** Relative amount of

chaperone:subunit complex (red) and subunit:Nte complex (blue) quantified at different times during DSE using ESI-MS.

Figure 3. Discrimination in pilus assembly revealed by the apparent rate of DSE of different cognate/ non-cognate chaperone:subunit Nte pairs. The apparent rate of DSE, monitored by the loss of chaperone:subunit complex *versus* time followed by nanoESI-MS for **(a)** PapD:PapG; **(b)** PapD:PapF; **(c)** PapD:PapE$_{Ntd1}$; **(d)** PapD:PapK; **(e)** PapD:PapA$_{Ntd1G15N}$ and **(f)** PapD:PapH$_{Ntd1}$ when challenged with F$_{Nte}$ (orange), E$_{Nte}$ (yellow), K$_{Nte}$ (green), A$_{Nte}$ (light blue) or H$_{Nte}$ (dark blue). The stability of each chaperone:subunit complex in the absence of Nte peptide is shown in black. Corresponding apparent pseudo-first order rate constants (k_{obs}) for each chaperone:subunit Nte pair are shown in **(g-k)**, with cognate interactions indicated (*). For reactions in which less than 20% of the substrate reacts within 14 days, upper limits for k_{obs} were estimated based on the extent of substrate loss at this time (hatched bars). Errors are given in SI Table 1.

Figure 4. Comparison of the reactivity of each chaperone:subunit complex with its cognate Nte(s). The apparent rate of DSE of each chaperone:subunit complex for all cognate reactions: PapD:PapG + F$_{Nte}$ (red), PapD:PapF + E$_{Nte}$ (orange), PapD:PapE$_{Ntd1}$ + E$_{Nte}$ (yellow), PapD:PapE$_{Ntd1}$ + K$_{Nte}$ (olive), PapD:PapK + A$_{Nte}$ (green), PapD:PapA$_{Ntd1G15N}$ + A$_{Nte}$ (light blue) and PapD:PapA$_{Ntd1G15N}$ + H$_{Nte}$ (dark blue), measured as the loss of the initial chaperone:subunit complex monitored by nanoESI-MS.

Figure 5. Chimeric peptides show that the rate of DSE is determined by the C-terminal half of the Nte. (a) Decrease in PapD:PapE$_{Ntd1}$ signal intensity when challenged with E$_{Nte}$ (yellow), H$_{Nte}$ (blue), E/H$_{Nte}$ (black) or H/E$_{Nte}$ (grey). Inset: Sequences of E$_{Nte}$, H$_{Nte}$, E/H$_{Nte}$

and H/E_{Nte}. **(b)** Decrease in PapD:PapF signal intensity when challenged with E_{Nte} (yellow), K_{Nte} (green), E/K_{Nte} (black) or K/E_{Nte} (grey). Inset: Sequences of E_{Nte}, K_{Nte}, E/K_{Nte} and K/E_{Nte}. In the sequences, the P2-P5 residues are highlighted in red.

References

1. Thanassi DG, Hultgren SJ (2000) Multiple pathways allow protein secretion across the bacterial outer membrane. *Curr Opin Cell Biol* 12: 420-430.
2. Stathopoulos C, *et al.* (2000) Secretion of virulence determinants by the general secretory pathway in gram-negative pathogens: an evolving story. *Microbes Infect* 2: 1061-1072.
3. Kuehn MJ, Heuser J, Normark S, Hultgren SJ (1992) P pili in uropathogenic E. coli are composite fibres with distinct fibrillar adhesive tips. *Nature* 356: 252-255.
4. Lindberg F, Lund B, Johansson L, Normark S (1987) Localization of the receptor-binding protein adhesin at the tip of the bacterial pilus. *Nature* 328: 84-87.
5. Thanassi DG, Saulino ET, Hultgren SJ (1998) The chaperone/usher pathway: a major terminal branch of the general secretory pathway. *Curr Opin Microbiol* 1: 223-231.
6. Jones CH, *et al.* (1997) The chaperone-assisted membrane release and folding pathway is sensed by two signal transduction systems. *EMBO J* 16: 6394-6406.
7. Soto GE, *et al.* (1998) Periplasmic chaperone recognition motif of subunits mediates quaternary interactions in the pilus. *EMBO J* 17: 6155-6167.
8. Sauer FG, Pinkner JS, Waksman G, Hultgren SJ (2002) Chaperone priming of pilus subunits facilitates a topological transition that drives fiber formation. *Cell* 111: 543-551.
9. Dodson KW, Jacob-Dubuisson F, Striker RT, Hultgren SJ (1993) Outer-membrane PapC molecular usher discriminately recognizes periplasmic chaperone-pilus subunit complexes. *Proc Natl Acad Sci U S A* 90: 3670-3674.
10. Sauer FG, Remaut H, Hultgren SJ, Waksman G (2004) Fiber assembly by the chaperone-usher pathway. *Biochim Biophys Acta* 1694: 259-267.
11. Holmgren A, Branden CI (1989) Crystal structure of chaperone protein PapD reveals an immunoglobulin fold. *Nature* 342: 248-251.
12. Sauer FG, *et al.* (1999) Structural basis of chaperone function and pilus biogenesis. *Science* 285: 1058-1061.
13. Choudhury D, *et al.* (1999) X-ray structure of the FimC-FimH chaperone-adhesin complex from uropathogenic Escherichia coli. *Science* 285: 1061-1066.
14. Zavialov AV, *et al.* (2003) Structure and biogenesis of the capsular F1 antigen from Yersinia pestis: preserved folding energy drives fiber formation. *Cell* 113: 587-596.
15. Remaut H, *et al.* (2006) Donor-strand exchange in chaperone-assisted pilus assembly proceeds through a concerted beta strand displacement mechanism. *Mol Cell* 22: 831-842.
16. Gong M, Makowski L (1992) Helical structure of P pili from Escherichia coli. Evidence from X-ray fiber diffraction and scanning transmission electron microscopy. *J Mol Biol* 228: 735-742.
17. Jacob-Dubuisson F, *et al.* (1993) Initiation of assembly and association of the structural elements of a bacterial pilus depend on two specialized tip proteins. *EMBO J* 12: 837-847.
18. Verger D, *et al.* (2006) Molecular mechanism of P pilus termination in uropathogenic Escherichia coli. *EMBO rep* 7: 1228-1232.
19. Roberts JA, *et al.* (1994) The Gal(alpha 1-4)Gal-specific tip adhesin of Escherichia coli P-fimbriae is needed for pyelonephritis to occur in the normal urinary tract. *Proc Natl Acad Sci U S A* 91: 11889-11893.
20. Saulino ET, Thanassi DG, Pinkner JS, Hultgren SJ (1998) Ramifications of kinetic partitioning on usher-mediated pilus biogenesis. *EMBO J* 17: 2177-2185.

21. Lee YM, Dodson KW, Hultgren SJ (2007) Adaptor function of PapF depends on donor strand exchange in P-pilus biogenesis of Escherichia coli. *J Bacteriol* 189: 5276-5283.
22. Benesch JL, Ruotolo BT, Simmons DA, Robinson CV (2007) Protein complexes in the gas phase: technology for structural genomics and proteomics. *Chem Rev* 107: 3544-3567.
23. Verger D, Bullitt E, Hultgren SJ, Waksman G (2007) Crystal structure of the P pilus rod subunit PapA. *PLoS Pathog* 3: e73.
24. Rose RJ, *et al.* (2008) Donor-strand exchange in chaperone-assisted pilus assembly revealed in atomic detail by molecular dynamics. *J Mol Biol* 375: 908-919.
25. Jacob-Dubuisson F, Striker R, Hultgren SJ (1994) Chaperone-assisted self-assembly of pili independent of cellular energy. *J Biol Chem* 269: 12447-12455.
26. Nishiyaman, M, Ishikawa, T, Rechsteiner, H & Glockshuber, R (2008) Reconstitution of pilus assembly reveals a bacterial outer membrane catalyst. *Science* 320: 376-379.
27. Remaut, H, Tang, C, Henderson, NS, Pinkner, JS, Wang, T, Hultgren, SJ, Thanassi, DG, Waksman G & Li, H (2008) Fiber formation across the bacterial outer membrane by the chaperone/usher pathway. *Cell* 133, 640-652.

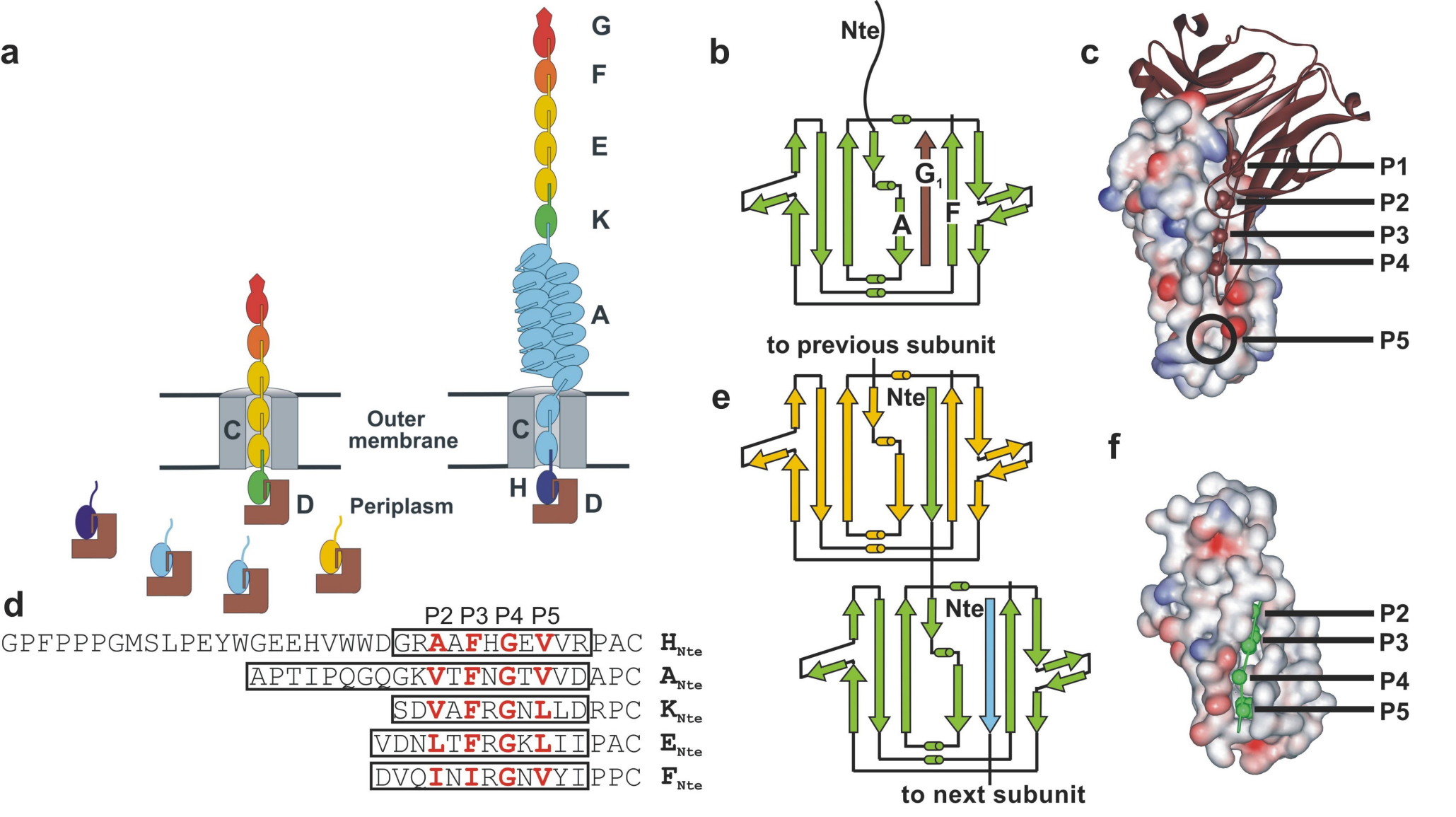
a
G
F
E
K
A
C
Outer membrane
C
D
Periplasm
H
D
b
Nte
G1
A
F
to previous subunit
c
P1
P2
P3
P4
P5
e
Nte
Nte
to next subunit
f
P2
P3
P4
P5
d
P2 P3 P4 P5
GPFPPPGMSLPEYWGEEHVWWDGRAAFHGEVVRPAC HNte
APTIPQGQGKVTFNGTVVDAPC ANte
SDVAFRGNLLDRPC KNte
VDNLTFRGKLIIPAC ENte
DVQINIRGNVYIPPC FNte

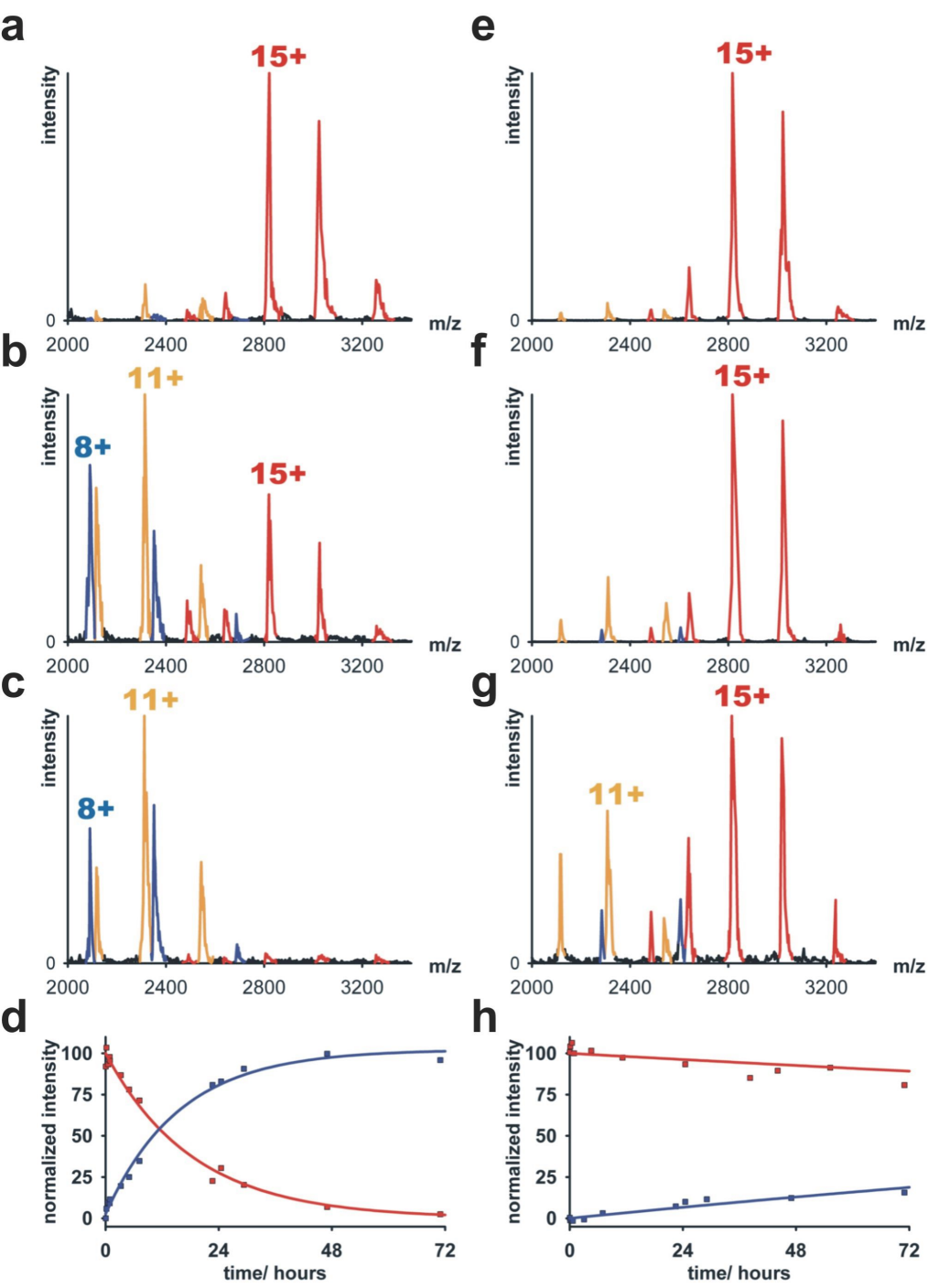
a
15+
intensity
0
m/z
2000
2400
2800
3200
b
11+
8+
15+
c
11+
8+
d
normalized intensity
100
75
50
25
0
24
48
72
time/ hours
e
15+
f
15+
g
15+
11+
h

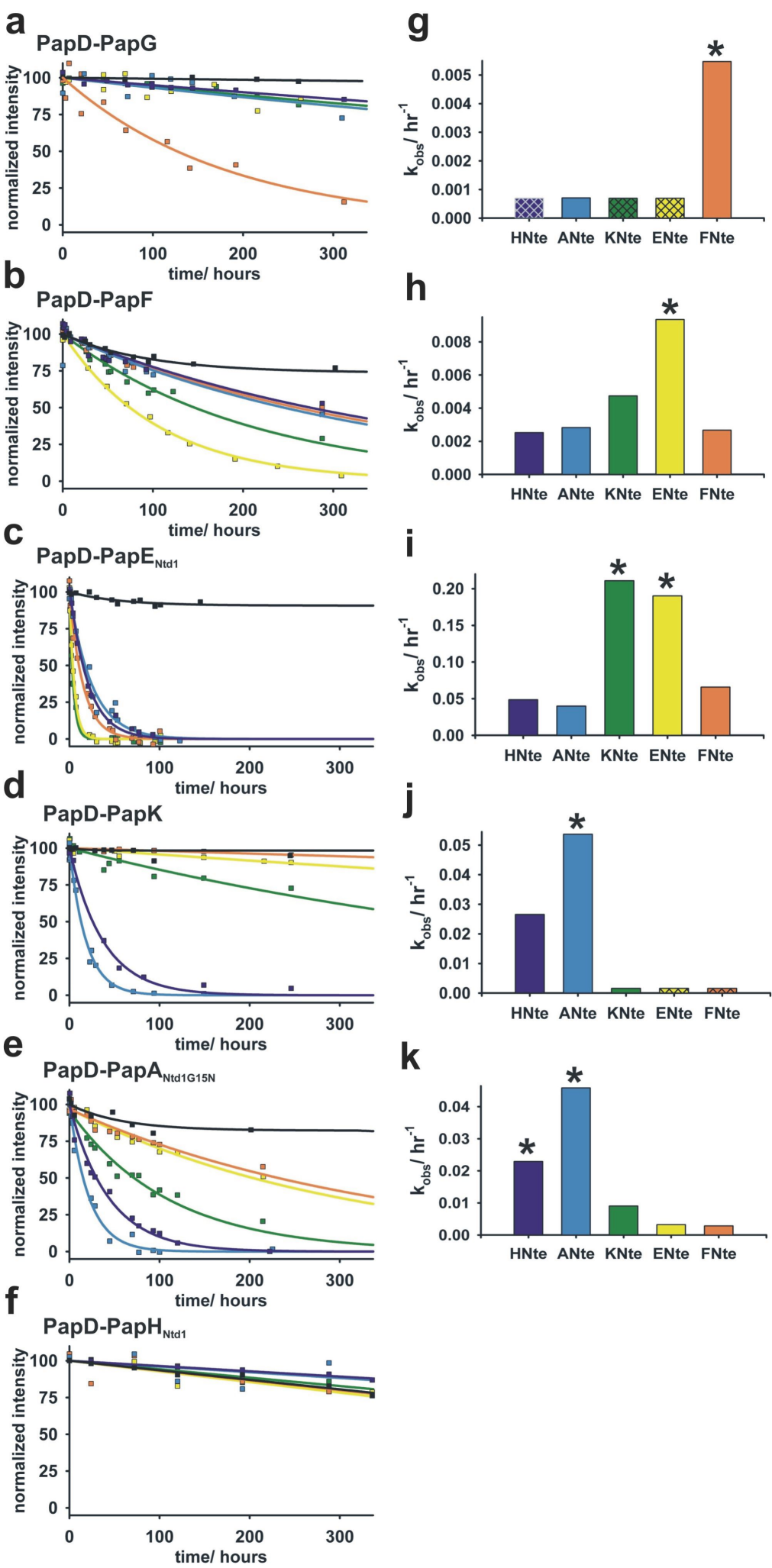
a
PapD-PapG
normalized intensity
time/ hours
b
PapD-PapF
normalized intensity
time/ hours
c
PapD-PapE$_{Ntd1}$
normalized intensity
time/ hours
d
PapD-PapK
normalized intensity
time/ hours
e
PapD-PapA$_{Ntd1G15N}$
normalized intensity
time/ hours
f
PapD-PapH$_{Ntd1}$
normalized intensity
time/ hours
g
k_{obs}/ hr^{-1}
HNte ANte KNte ENte FNte
h
k_{obs}/ hr^{-1}
HNte ANte KNte ENte FNte
i
k_{obs}/ hr^{-1}
HNte ANte KNte ENte FNte
j
k_{obs}/ hr^{-1}
HNte ANte KNte ENte FNte
k
k_{obs}/ hr^{-1}
HNte ANte KNte ENte FNte

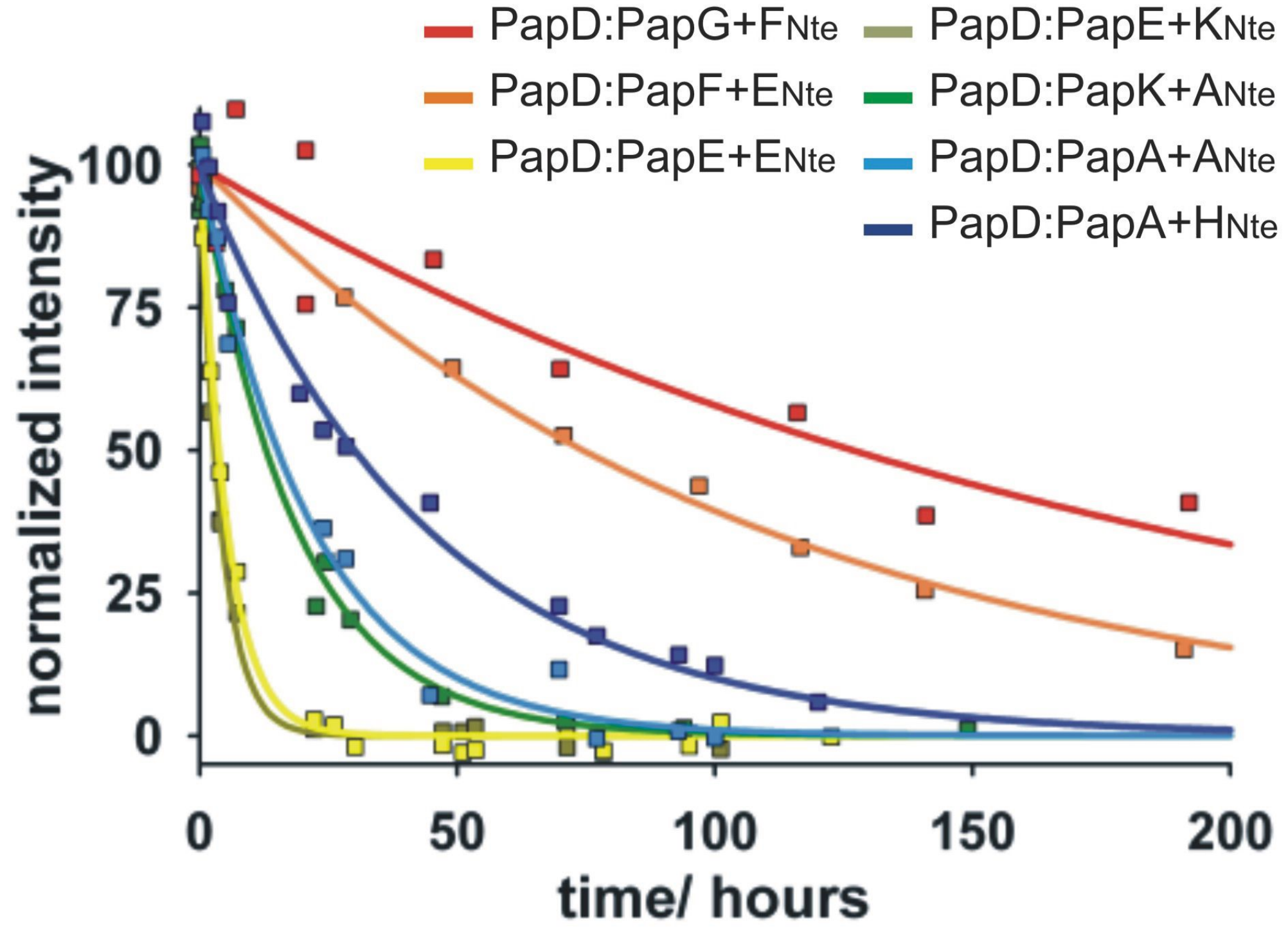
PapD:PapG+FNte
PapD:PapF+ENte
PapD:PapE+ENte
PapD:PapE+KNte
PapD:PapK+ANte
PapD:PapA+ANte
PapD:PapA+HNte
normalized intensity
100
75
50
25
0
0
50
100
150
200
time/ hours

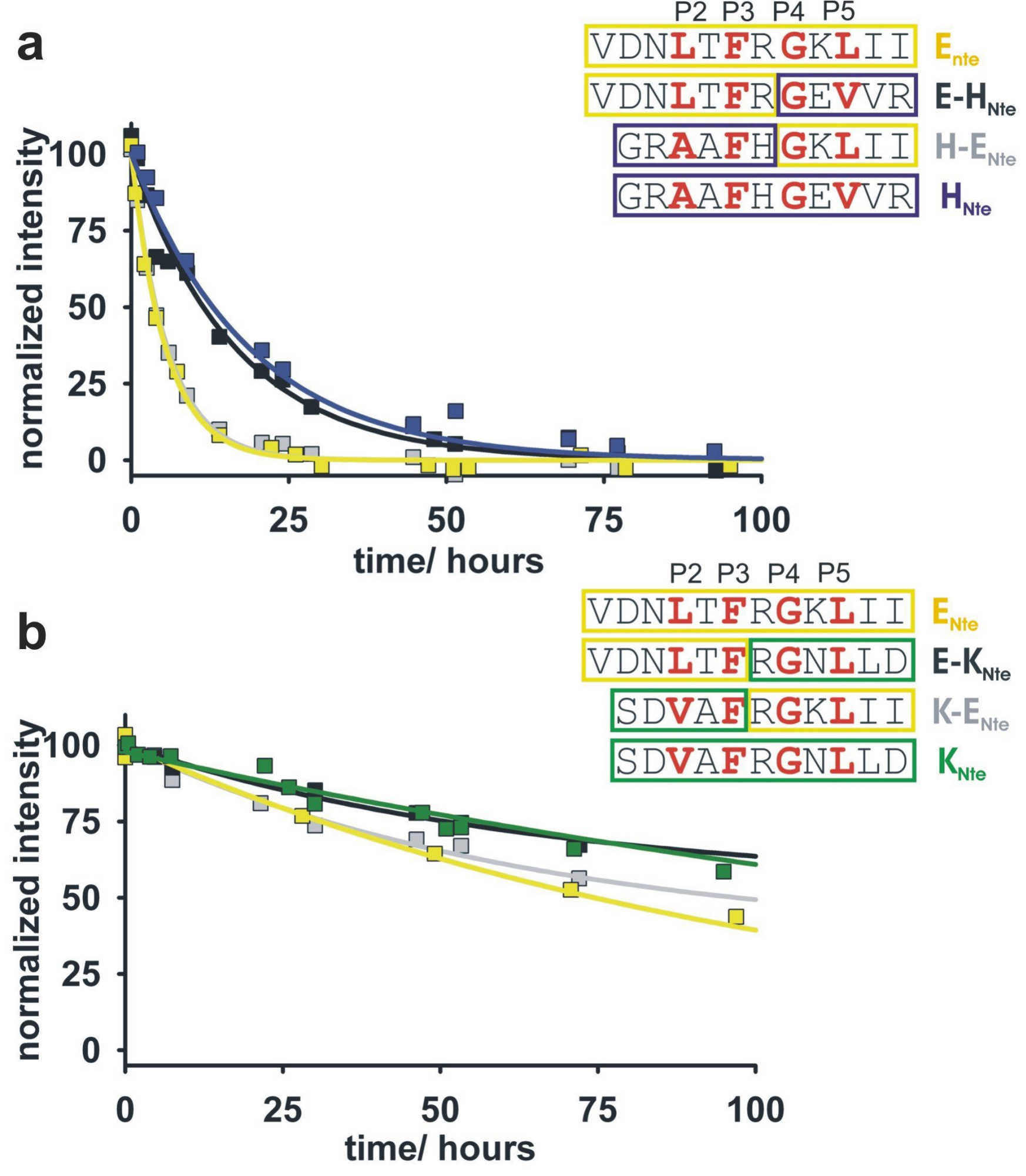
a
P2 P3 P4 P5
VDNLTFRGKLII
E_nte
VDNLTFRGEVVR
E-H_Nte
GRAAFHGKLII
H-E_Nte
GRAAFHGEVVR
H_Nte
normalized intensity
100
75
50
25
0
0
25
50
75
100
time/ hours
b
P2 P3 P4 P5
VDNLTFRGKLII
E_Nte
VDNLTFRGNLLD
E-K_Nte
SDVAFRGKLII
K-E_Nte
SDVAFRGNLLD
K_Nte
normalized intensity
100
75
50
25
0
0
25
50
75
100
time/ hours